

# Impact of phytoplankton and bacterial production on nutrient and DOM uptake in the Rhône River plume (NW Mediterranean)

Mireille Pujo-Pay\*, Pascal Conan, Fabien Joux, Louise Oriol, Jean Jacques Naudin, Gustave Cauwet

Laboratoire d'Océanographie Biologique de Banyuls, CNRS-UMR 7621-Université de Paris 6, Laboratoire Arago, BP 44, 66651 Banyuls-sur-Mer, Cedex, France

**ABSTRACT:** From April 1998 to April 1999, 4 cruises were conducted to investigate the evolution of physical and biological characteristics of the Rhône River plume. Particular emphasis was placed on the relationships between phytoplanktonic or bacterial production and environmental conditions. For most of the year, distributions of nutrients, phytoplankton and bacterial activities were conservative along the salinity gradient, indicating the dominance of physical dilution processes. In April 1999, nutrient-salinity relationships showed strong deviations from the conservative mixing line which were associated with a phytoplankton bloom. Deviations from the conservative mixing line were used to estimate the relative contributions of physical and biological processes in the removal of riverine derived material. During the phytoplankton bloom, there was a specific organisation of the microbial populations and their activities at intermediate salinity. Maximal productions were associated with maxima in ammonium and phosphate uptake rates for bacteria, but with maxima in nitrate uptake rates for phytoplankton. The relative accumulation of dissolved organic carbon (DOC) and nitrogen (DON) at high salinity, and the seasonal variability in their distribution, resulted in a potential competition between bacteria and phytoplankton for key mineral nutrients highlighted by an increase in the DOC:DON ratio up to 10. This study contributes to our understanding of the relationship between phytoplankton, bacteria and dissolved organic matter and helps to elucidate the factors controlling the productivity of the system. In particular, the impact of wind and riverine output need to be considered alongside seasonal variability in the chemical and hydrodynamic environment.

**KEY WORDS:** Rhône River plume · Dilution area · Estuaries · Nutrient uptake · DOM uptake · Primary production · Bacterial production

*Resale or republication not permitted without written consent of the publisher*

## INTRODUCTION

There has been growing concern over the effects of dissolved material inputs on the coastal margins of the European seas, as establishing the fate of this material is essential for predicting the effects of climate change and other anthropogenic alterations. The Rhône River discharges large quantities of nutrients into the coastal zone of the NW Mediterranean which influences the nature and the rates of processes occurring in the recipient sediment and water column. The Rhône has many anthropogenic inputs along its course to the Mediterranean, including diverse industrial discharges, out-

flows from sewage plants, and runoff from agricultural regions. Large quantities of nitrogen, phosphorus, and carbon are stored and transported as organic and inorganic matter (in the dissolved phase) in terrestrial water discharge. The Rhône contributes only 0.1% of the regions total water flux, but contributes 1% of the dissolved organic carbon (DOC) flux ( $3 \times 10^{10}$  mol yr<sup>-1</sup>, Yoro et al. 1997), and 50% of the nutrient flux ( $1 \times 10^8$  mol yr<sup>-1</sup> for PO<sub>4</sub> and from  $4 \times 10^9$  to  $7 \times 10^9$  mol yr<sup>-1</sup> for NO<sub>3</sub>, Conan et al. 1998). Inputs may support 50 to 70% of the new production for the whole Gulf of Lion (Lefèvre et al. 1997) and their variations may change the growth and behaviour of phytoplankton. The stimu-

\*Email: pujopay@obs-banyuls.fr

latory effect of the high nutrient concentrations may be damped by the high particulate loading associated with the river plume, this results in a reduction of the light available to the phytoplankton and hence tends to inhibit growth. Furthermore, dissolved organic matter (DOM) is the major light absorbing agent in coastal waters. Transparency and heat budgets for the coastal areas are thus modified and controlled by DOM, and aquatic primary producers compete with DOM for available light. The mouth and the plume of the Rhône River contains high levels of nutrients while the dilution area exhibits the highest levels of primary production, including a large diatom spring bloom (Minas & Minas 1989, Lefèvre et al. 1997). Analysis of a 30 yr data set for the Gulf of Lion revealed that net community production (NCP) is nearly in balance, except in April during the spring bloom when NCP is strongly positive (Lefèvre et al. 1997).

The coastal margins of the Gulf of Lion exhibit complex hydrological events where several intense and highly variable physical processes interact (circulation, thermo-haline convection, seasonal stratification combined with aperiodic mixing events associated with wind speed, Conan & Millot 1995). Regional models (e.g. Estournel et al. 2001, Arnoux-Chiavassa & Fraunié 2003) describe the hydrodynamical variability of the Rhône River plume as a function of physical environmental conditions, but general ecosystem functioning remains poorly defined. The effect of riverine inputs on the coastal area influenced by the Rhône is complex and requires further investigation to define the role of nutrients in eutrophication and to quantify

the real impact of the rivers in the Mediterranean Sea, especially in the Gulf of Lion.

The overall aim of this project was to further resolve the riverine export of dissolved organic and inorganic matter, and its fate and impacts on coastal ecosystem functioning, i.e. the storage and cycling of carbon and nitrogen. During 4 cruises, from April 1998 to May 1999, studies were conducted to investigate the evolution of physical and biological characteristics of the Rhône plume. This paper focuses on regional biogeochemistry, particularly the influence of environmental forcings on the organisation of the pelagic ecosystem (phytoplankton and bacteria) between the Rhône River mouth and the dilution area. Our results define the role of the spring bloom (April 1999) on dilution processes of the Rhône inputs.

## MATERIALS AND METHODS

**Sampling strategy.** Four Biodypar (Biogéochimie et Dynamique du Panache du Rhône) cruises were conducted between April 1998 and April 1999 (Biodypar 1 in April 1998, Biodypar 2 in November 1998, Biodypar 3 in March 1999, and Biodypar 4 in April 1999) in the Rhône plume, i.e. the coastal area under riverine influence. The sampling strategy for biogeochemical analyses was based on the Lagrangian motion of a surface drifter already described by Naudin et al. (2001). The drifter was designed to follow the water movement of the plume. Resultant trajectories were dependent on the prevailing meteorological conditions during each cruise (Fig. 1). During the Biodypar Cruise 4, the 2 trajectories were studied, D112 and D120. The drifter was released 1 mile southeast of the Rhône River mouth and then tracked by the ship. In this manner, our sampling could account for both spatial and temporal variability in the discharge of material. While following the drifter, samples were collected in the plume and in the underlying marine water. Subsurface samples were collected at 0.5, 1, 2, and 3 m depths using a vacuum pump which transferred water (through Teflon tubing), directly from the respective *in situ* depth, to shipboard glass (5 l) or polycarbonate bottles (20 l). For this purpose, a weighted polystyrene floating plate connected to the ship with Teflon tubes permitted sampling away from any influence of the ship, with minimum effects on the structure of the halocline (see Naudin et al. 2001 for details). A deeper sample (10 m) was collected with a 5 l Niskin bottle and was used as a marine water reference.

CTD measurements of conductivity, temperature, turbidity, and fluorescence (as functions of depth) were made from the ship using an EcoProb probe (Meeres-technik Elektronik). Accurate salinity measurements

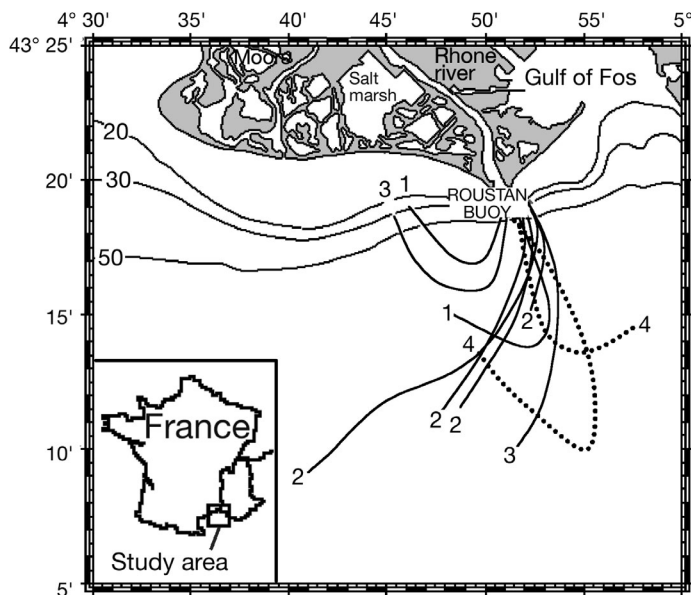


Fig. 1. Location of the trajectories described by the drifter in the Rhône River plume during the Biodypar Cruises 1, 2, 3 and 4

were also performed at the land laboratory using a Guildline 8410 portable salinometer (accuracy  $\pm 0.01$ ).

**Nutrient analysis.** Samples for inorganic nutrients were immediately filtered (ashed Whatman GF/F filter) on board after sampling. For ammonia ( $\text{NH}_4$ ) determination, reagents were immediately added to subsamples filtered in glass bottles. Measurements were then performed with a spectrophotometer (Spectronic 401) according to the Koroleff's manual method (1969). Measurement accuracy ranged between 0.020 and 0.075  $\mu\text{M}$ . Samples for nitrate+nitrite ( $\text{NO}_3$ ) and phosphate ( $\text{PO}_4$ ) determinations were frozen ( $-20^\circ\text{C}$ ) immediately on board in polyethylene bottles until further analyses in the laboratory. They were analysed according to Tréguer & Le Corre (1975) on a Skalar auto-analyser. Measurement accuracy was  $\pm 0.1$ ,  $\pm 0.02$  and  $\pm 0.02$   $\mu\text{M}$  for  $\text{NO}_3$ ,  $\text{NO}_2$  and  $\text{PO}_4$  respectively.

**Dissolved organic matter.** Samples for DOM (dissolved organic nitrogen, DON; phosphorus, DOP; and carbon, DOC) were filtered through 2 precombusted (24 h,  $450^\circ\text{C}$ ) glass fibre filters (Whatman GF/F 25 mm). Samples for DON and DOP were collected directly in Teflon bottles and immediately frozen on board ( $-20^\circ\text{C}$ ) and stored for later analyses. DON and DOP were simultaneously determined by the wet oxidation procedure described in Pujo-Pay & Raimbault (1994) and Pujo-Pay et al. (1997). DON ( $\pm 0.1$   $\mu\text{M}$ ) and DOP ( $\pm 0.02$   $\mu\text{M}$ ) concentrations, were determined by sample oxidation (30 min,  $120^\circ\text{C}$ ) corrected for  $\text{NH}_4$ ,  $\text{NO}_3+\text{NO}_2$  and  $\text{PO}_4$  concentrations, respectively. DOC samples were collected and stored in precombusted glass tubes closed with a screw cap and a Teflon liner. Each tube was poisoned with mercuric chloride ( $5 \text{ mg l}^{-1}$ ) and stored at room temperature until analysis. DOC was analysed using the high temperature catalytic oxidation (HTCO) technique (Sugimura & Suzuki 1988, Cauwet 1994) using a Shimadzu TOC-5000 analyser.

**Chlorophyll.** Samples for chlorophyll biomass (total chlorophyll) were filtered onto GF/F filters and kept on board in liquid nitrogen for later analyses. Chlorophyll concentration was determined using a PERKIN-ELMER MPF 66 spectrofluorometer following the method of Neveux & Panouse (1987).

**Primary production.** Primary production was determined using the  $^{14}\text{C}$ -tracer technique (Steemann-Nielsen 1952) modified by Fitzwater et al. (1982). Sample water was dispensed into triplicate acid cleaned (0.5 N HCl) 250 ml polycarbonate bottles and 1 dark bottle. After sampling, 0.25 ml of  $\text{Na}_2\text{H}^{14}\text{CO}_3$  working solution was added to each bottle (final activity  $\sim 0.07$   $\mu\text{Ci ml}^{-1}$ ). Total added activity was assayed on a 250  $\mu\text{l}$  aliquot collected in a scintillation vial containing 250  $\mu\text{l}$  of ethanolamine. Samples were then incubated under simulated *in situ* conditions for 24 h in a deck

incubator cooled by surface sea water. In order to simulate subsurface irradiance, incubators were covered by a screen which removed 50% of the incident sunlight. At the end of incubation, samples were filtered onto Whatman GF/F filters (25 mm diameter) under low pressure ( $< 100$  mm Hg), rinsed with 500  $\mu\text{l}$  of 0.5 N HCl, placed into scintillation vials and dried at  $40^\circ\text{C}$  for 12 h. At the laboratory, 10 ml of a liquid scintillation cocktail (Aquasol) were added to all scintillation vials before counting with a Beckman Scintillation Counter. Total carbonate concentration was calculated according to Parsons et al. (1992) and carbon assimilation rates were calculated according to Platt & Sathyendranath (1993).

**Bacterial abundance and production.** Bacteria were counted with a FACScan flow cytometer (Becton Dickinson). Samples were fixed with 2% formaldehyde and frozen immediately on board in liquid nitrogen and stored at  $-80^\circ\text{C}$  until their analysis. Before analysis, bacteria were stained with SYBR Green II (final concentration 0.05% [vol/vol] of the commercial solution; Molecular Probes) for at least 15 min at  $20^\circ\text{C}$  in the dark, and analyzed with the cytometer. Bacteria were detected by their signatures in a plot of green fluorescence (collected through a  $530 \pm 30$  nm band pass filter) versus right angle light scatter. Bacterial production was determined by [ $^3\text{H}$ -methyl] thymidine ( $^3\text{HTdR}$ ) incorporation (Fuhrman & Azam 1982). Duplicate samples (10 ml) were incubated in the presence of a saturating concentration of  $^3\text{HTdR}$  (40 nM final concentration; specific activity of 64 Ci  $\text{mmol}^{-1}$ ; IsotopChim) for 2 h at *in situ* temperatures in the dark. Then, samples were fixed by addition of trichloroacetic acid (TCA) (5% final concentration), filtered onto 0.2  $\mu\text{m}$  pore-size membrane filters (GSWP, Millipore) and rinsed twice with 5% TCA. Filters were dissolved with liquid scintillation cocktail (FilterCount, Packard) and then radioassayed (LS 5000CE, Beckman scintillation counter). Incorporation rates were corrected for abiotic adsorption of  $^3\text{HTdR}$  measured in killed samples (i.e. addition of 5% TCA before  $^3\text{HTdR}$ ). Rates of thymidine incorporation were converted to bacterial carbon production using the conversion factor of  $0.5 \times 10^{18}$  cell  $\text{mol}^{-1}$  of incorporated thymidine (Servais & Lavandier 1995), and using a cell-to-carbon conversion factor of 20 fg C cell $^{-1}$  (Lee & Fuhrman 1987).

## RESULTS

### General environmental conditions

During the study period, the spatial extent and location of the Rhône plume (thus specific locations of the drifter trajectories, Fig. 1) was largely driven by wind

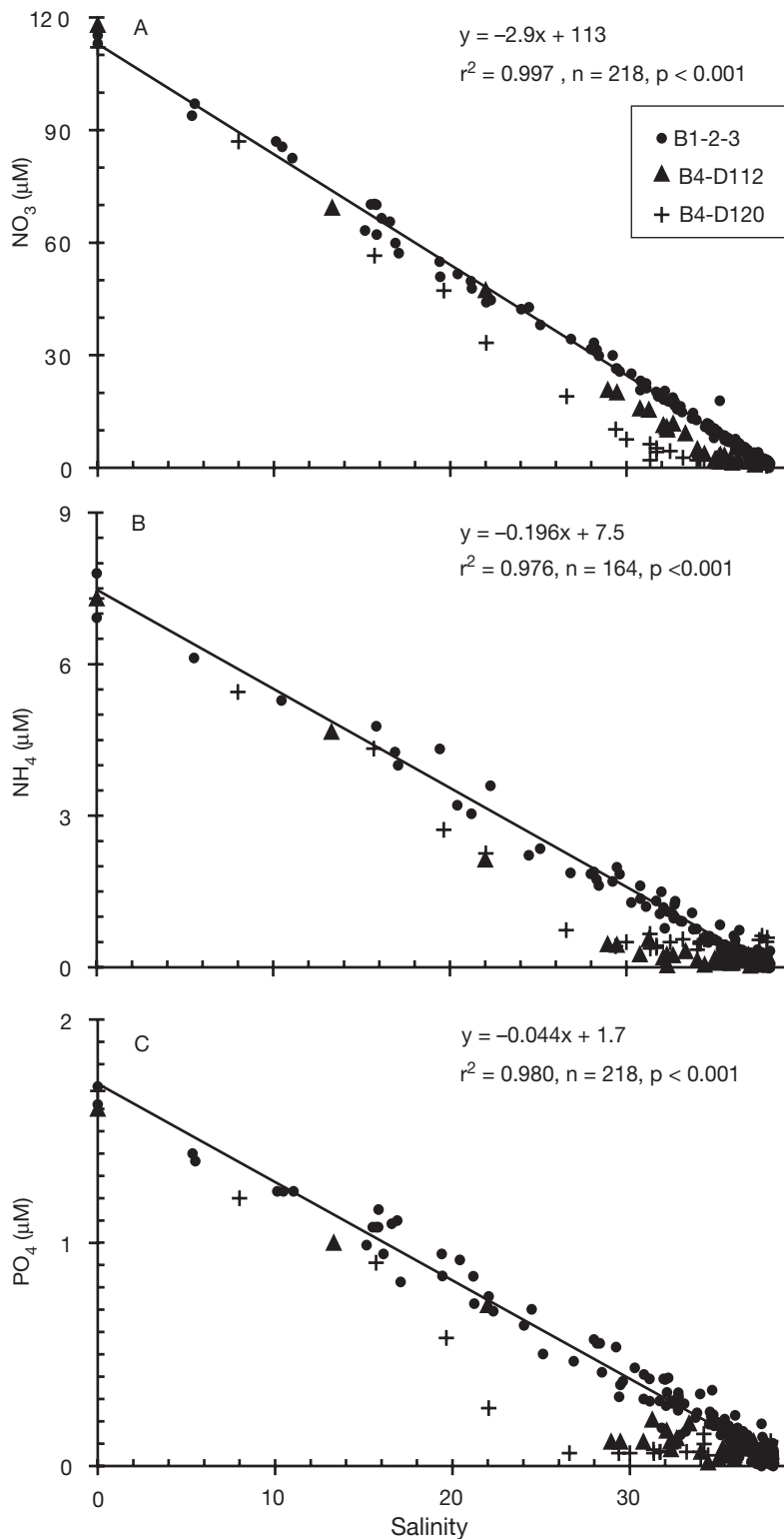


Fig. 2. Concentrations of (A) nitrate+nitrite ( $\text{NO}_3$ ), (B) ammonium ( $\text{NH}_4$ ), and (C) phosphate ( $\text{PO}_4$ ) versus salinity plot in the Rhône River plume. All data are pooled for Biodypar Cruises 1, 2, and 3 (B1-2-3) to fit a high significant least-square regression (formula and statistics indicated on each panel). Data for the Biodypar 4 Cruise are used separately to calculate a net nutrient uptake (see text for details), data for 2 trajectories, D112 and D120, are shown

conditions and river discharge. Trajectories were generally oriented in a south-westerly direction when dominant winds were blowing from land, whereas dominance by onshore winds (which influenced the balance between the Coriolis and inertial forces) resulted in a more landward trajectory. Under all conditions encountered during the different cruises, the river flow was found to decrease gradually with distance from the river mouth whilst salinity was characterised by a steep gradient and vertical salinity stratification was always present in surface waters (0 to 10 m). Depending on the river discharge and wind velocity, the depth of the river plume varied from less than 1 to 2 m. Description and analysis of similar trajectories can be found in Naudin et al. (2001).

### Nutrients

A consistent evolution in the distribution of key nutrients ( $\text{NO}_3$ ,  $\text{NH}_4$ ,  $\text{PO}_4$ ) was observed with water flow. As with salinity, the general trend for nutrient concentrations was a decrease with increasing depth and distance from the river mouth. The conservative and non-conservative fractions of nutrients in a seawater sample can be calculated from a mixing line superimposed on a nutrient-salinity plot of a suite of oceanographic data (Fig. 2). The mixing line reflects the change in nutrient concentration that would occur if neither biological nor chemical processes (adsorption, degradation, scavenging, etc.) influenced the mixing of the 2 water masses. For example, the nutrient concentration ( $C_{\text{mix}}$ ) of a water mass of salinity ( $S_{\text{mix}}$ ) resulting from exclusively mixing of 2 water masses (one with salinity,  $S_A$ , and nutrient concentration,  $C_A$ , and one with salinity,  $S_B$ , and nutrient concentration,  $C_B$ ) can be simply deduced from the expression:

$$C_{\text{mix}} = C_A \times (S_{\text{mix}} - S_B) / (S_A - S_B) + C_B \times (S_A - S_{\text{mix}}) / (S_A - S_B)$$

Departure of the measured concentration from its theoretical location on the mixing line reflects the combined effects of consumption by phytoplankton and/or

bacteria ( $-\Delta\text{NO}_3$ ,  $-\Delta\text{NH}_4$ ,  $-\Delta\text{PO}_4$ ), denitrification or nitrification by bacteria ( $-\Delta\text{NO}_3$ ,  $-\Delta\text{NH}_4$ ), bacterial and/or zooplankton excretion ( $+\Delta\text{NH}_4$ ,  $+\Delta\text{PO}_4$ ), mineralization by bacteria ( $+\Delta\text{NO}_3$ ,  $+\Delta\text{PO}_4$ ), adsorption, and sedimentation (preferentially  $-\Delta\text{PO}_4$ ). This latter process is known to be weak in the Rhône plume (Coste 1974). The measured nutrient concentration of a sample taken in the dilution zone is thus a net budget of all these antagonistic processes and we consider that negative values of  $C_{\text{mix}}$  reflect a biological uptake whilst positive values of  $C_{\text{mix}}$  represent the production or release of the considered element.

Thus, the  $\text{NO}_3$ ,  $\text{NH}_4$ , and  $\text{PO}_4$  anomalies ( $\Delta$ ) are calculated from the data of the nutrient-salinity physical mixing models, showed in Fig. 2, derived during Biodypar Cruises 1, 2, and 3. In our conceptual dilution model, freshwater comes from the Rhône, with a salinity of 0 and  $\text{NO}_3$ ,  $\text{NH}_4$ , and  $\text{PO}_4$  concentrations of 113, 7.5, and 1.7  $\mu\text{M}$ , respectively. It mixes with coastal surface seawater with a salinity of about 38 and no nutrients (or below the detection limit of measurement). These values serve as the limits for the mixing lines in Fig. 2.

During the 4 Biodypar cruises, the concentrations of  $\text{NO}_3$ ,  $\text{PO}_4$  and  $\text{NH}_4$  showed the same kind of pattern along the salinity gradient. Specifically, nutrient concentrations were high in low salinity waters and close to detection limits of measurements in high salinity waters (Fig. 2). For Biodypar Cruises 1, 2, and 3, property-salinity plots exhibited no consistent trend across the salinity gradient and all data were pooled to fit a highly significant regression line, similar to those defined in the physical dilution model (see Fig. 2 for regression formulae). Data collected during the Biodypar Cruise 4 (during the 2 trajectories D112 and D120) deviated from the regression mixing line. This deviation increased from trajectory D112 to D120 (Fig. 2A,C), except for  $\text{NH}_4$  (Fig. 2B).

If we consider the regression fit obtained from Biodypar Cruises 1, 2, and 3 as a reference for simple physical evolution of dissolved material in the river plume, property-salinity plots for Biodypar Cruise 4 indicate a depletion of nutrients relative to conservative mixing at intermediate and high salinities. Thus, from data plotted in Fig. 2, one can calculate the net  $\text{NO}_3$ ,  $\text{PO}_4$ , and  $\text{NH}_4$  uptake during the Biodypar Cruise 4. In the plot of nutrient uptake as a function of salinity (Fig. 3), the maximum  $\text{NO}_3$  uptake appeared at a salinity of 35 for D112 and of 31.5 for D120. It is also noticeable that maximum uptake of both  $\text{PO}_4$  and  $\text{NH}_4$  were shifted to lower salinity (about 29 for D112 and about 26 to 27 for D120). The general pattern for all nutrients was negligible uptake at low salinity, an increase in uptake between salinities of 20 to 35, and then a sharp decrease in uptake at the high salinity end of the gradient (Fig. 3).

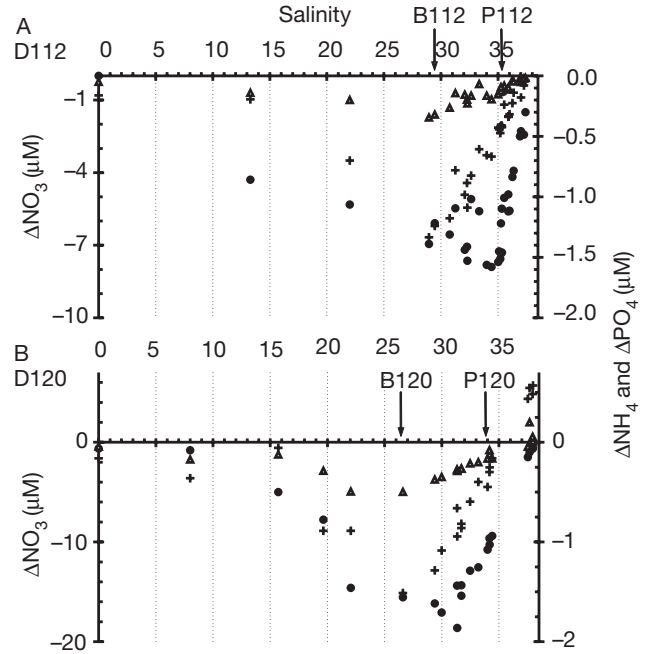


Fig. 3. Nutrient uptakes along the salinity in the Rhône River plume for Biodypar Cruise 4 for trajectories (A) D112 and (B) D120. Left scale = full dot for nitrate+nitrite ( $\Delta\text{NO}_3$ ). Right scale = cross for ammonium ( $\Delta\text{NH}_4$ ) and triangle for phosphate ( $\Delta\text{PO}_4$ ). The uptakes are calculated from the difference between the measured concentration and the theoretical concentration deduced from the conservative mixing line showed in Fig. 2 (see details in the text). The arrows indicate the maxima of biomass and production (shown in Fig. 4) for phytoplankton (P112 and P120) or bacteria (B112 or B120) for trajectories D112 or D120, respectively

Integration of nutrient uptakes along the salinity gradient indicates a net consumption during the dilution processes for each trajectory. A total amount of 64, 12.3, and 5.6  $\mu\text{M}$  for  $\text{NO}_3$ ,  $\text{NH}_4$ , and  $\text{PO}_4$ , respectively, disappeared due to processes other than simple physical dilution during the D112 cruise (Table 1). These amounts were higher during the D120 cruise and reached 103, 19.2 and 9.1  $\mu\text{M}$  for  $\text{NO}_3$ ,  $\text{NH}_4$  and  $\text{PO}_4$  respectively.

### Chlorophyll, primary productivity, bacterial abundance and production

As a general trend for all trajectories of Biodypar Cruises 1, 2, 3, and 4, but especially for Biodypar Cruise 4 where biological activity was significantly enhanced, we observed low biomass and production near the mouth of the river, a slow increase along the salinity gradient to reach maxima at intermediate salinities, and a drastic drop at the highest salinities (Fig. 4). This result is consistent with earlier obser-

vations in similar areas of riverine mixing (Davies 2004, Wawrik & Paul 2004). For Biodypar Cruise 4, there was a highly significant linear relationship between biomass and production for phytoplankton (Fig. 5A,  $r^2 = 0.83$ ,  $p < 0.001$ ) and bacteria (Fig. 5B,  $r^2 = 0.54$ ,  $p < 0.001$ ). The same kind of linear regression was encountered for the 2 trajectories, but maxima were located at salinities of 35.5 for phytoplankton and 29.5 for bacteria during D112, and at salinities of 34 and 26.5 during D120 (Fig. 4). Compared to the other cruises (Biodypar Cruises 1 to 3), the values of these maxima during the spring bloom were significantly higher and occurred in regions of lower salinity.

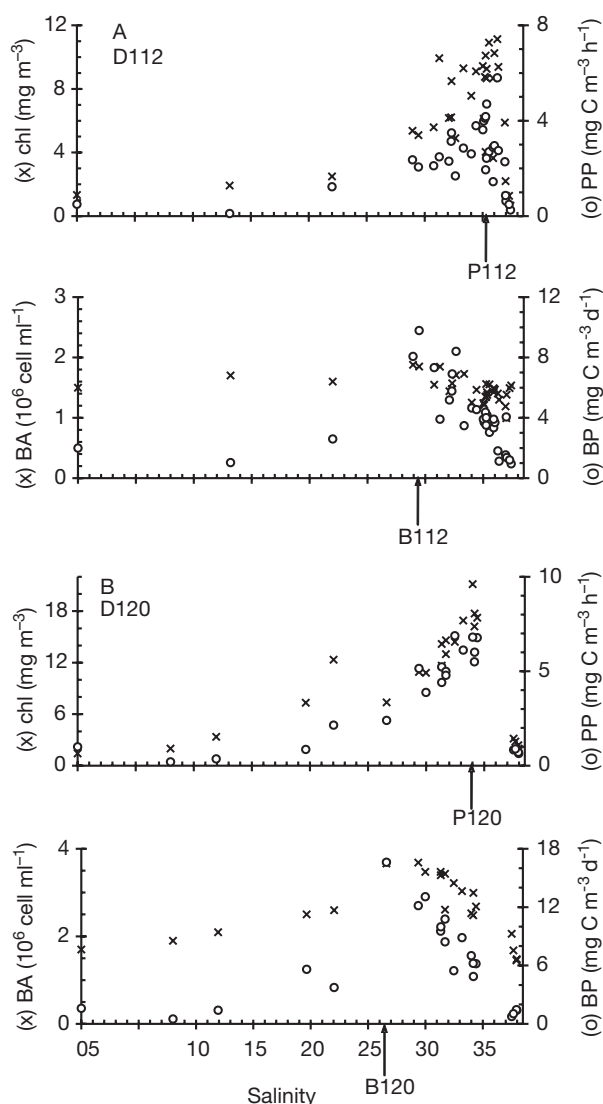


Fig. 4. Chlorophyll (chl), primary production (PP), bacterial abundance (BA) and production (BP) along the salinity gradient in the Rhône River Plume during the Biodypar Cruise 4 trajectories (A) D112 and (B) D120. For trajectories D112 or D120 arrows indicate maxima (reported in Fig. 3) phytoplankton (P112 or P120) and bacteria (B112 and B120)

Table 1. Integrated uptakes of NO<sub>3</sub> ( $\Delta$ NO<sub>3</sub>), NH<sub>4</sub> ( $\Delta$ NH<sub>4</sub>) and PO<sub>4</sub> ( $\Delta$ PO<sub>4</sub>), along the salinity gradient for Biodypar Cruise 4 (trajectories D112 and D120), calculated from the differences between measured concentrations and theoretical concentrations (derived from the conservative mixing line). The ratios of integrated uptakes ( $\Delta$ NO<sub>3</sub>: $\Delta$ PO<sub>4</sub>,  $\Delta$ NH<sub>4</sub>: $\Delta$ PO<sub>4</sub>, and ( $\Delta$ NO<sub>3</sub>+ $\Delta$ NH<sub>4</sub>): $\Delta$ PO<sub>4</sub>) are also calculated

$\mu$ M	D112	D120
$\Delta$ NO <sub>3</sub>	64	103
$\Delta$ NH <sub>4</sub>	12.3	19.2
$\Delta$ PO <sub>4</sub>	5.6	9.1
$\Delta$ NO <sub>3</sub> / $\Delta$ PO <sub>4</sub>	<b>11</b>	<b>11</b>
$\Delta$ NH <sub>4</sub> / $\Delta$ PO <sub>4</sub>	<b>2.2</b>	<b>2.1</b>
( $\Delta$ NO <sub>3</sub> + $\Delta$ NH <sub>4</sub> )/ $\Delta$ PO <sub>4</sub>	<b>14</b>	<b>13</b>

During the Biodypar Cruise 4 chlorophyll concentrations, as high as 18 mg m<sup>-3</sup> between salinities of 33 and 36, were 3 to 6 times higher (for D112 and D120 respectively) than during the other cruises (<4 mg m<sup>-3</sup>). On an aerial basis, mean primary production ranged from 90 to 150 mg C m<sup>-2</sup> d<sup>-1</sup>. Low values were found in November (Biodypar Cruise 2) and remained low during other cruises, except during April 1999 (Biodypar Cruise 4) during the phytoplankton bloom when values were close to 400 mg C m<sup>-2</sup> d<sup>-1</sup> for D120.

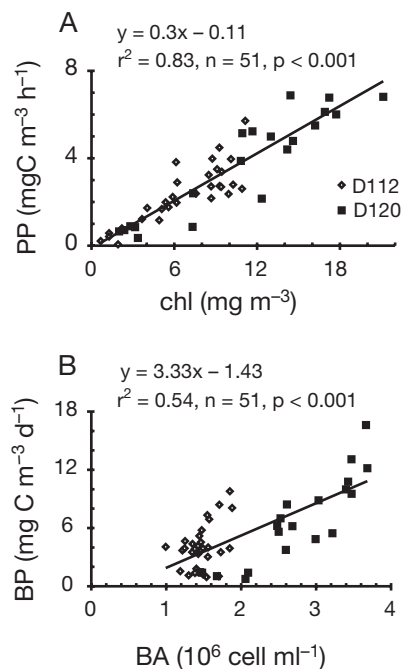


Fig. 5. Relationship between (A) chlorophyll (chl) and primary production (PP) and (B) bacterial abundance (BA) and bacterial production (BP) during the Biodypar Cruise 4 for trajectories D112 and D120. Data fit a highly significant linear least-square regression (formula and statistics are indicated on each panel)

### Relationship between nutrient uptake and biological activities

In order to investigate the relationship between nutrient utilisation and primary production and/or bacterial production in the dilution area, we compared the distribution of  $\Delta\text{NO}_3$ ,  $\Delta\text{NH}_4$ , and  $\Delta\text{PO}_4$  (Fig. 3) with biomass and productivity (Fig. 4). The evolution of nutrient uptake along the salinity gradient showed the same pattern as for biomass and activity, i.e. low values at low salinity which increased to a maximum at intermediate salinities and then decreased sharply at high marine salinity. The uptake of  $\text{NH}_4$  and  $\text{PO}_4$  were slightly different from  $\text{NO}_3$  uptake. Indeed, if the total increase of nutrient uptake between D112 and D120 was approximately 60% for all nutrients (Table 1), then the positive values of  $\Delta\text{NH}_4$  and  $\Delta\text{PO}_4$  at the end of the gradient (coastal marine water) indicate 'production' rather than removal of these nutrients (Figs. 3 & 6). When comparing Figs. 3 & 4, the maximum phytoplankton biomass and production were spatially coincident with the highest nitrate consumption rate for both cruises (arrows in Fig. 3). In contrast, bacterial abundance and production were spatially coincident with the highest  $\text{NH}_4$  and  $\text{PO}_4$  consumption rates. This was supported by a highly significant linear relationship between primary production and  $\Delta\text{NO}_3$ . There were similar relationships between bacterial production and  $\Delta\text{NH}_4$  and  $\Delta\text{PO}_4$  (Fig. 6).

### Distribution of dissolved organic matter

As for nutrients, the general pattern for DOC, DON and DOP was a linear decrease along the salinity gradient according to physical dilution processes. The dilution processes explained from 83 to 98% of the total DOC variability (maximum during Biodypar Cruises 1, 2, and 3, and minimum during Biodypar Cruise 4). It is also possible to define a theoretical conservative mixing line between characteristics of riverine (9.3, 0.38 and 178  $\mu\text{M}$  for DON, DOP and DOC, respectively) and marine (5, 0, and 50  $\mu\text{M}$  for DON, DOP and DOC, respectively) waters (Fig. 7). Finally, a potential uptake and/or production was deduced from the difference between measured DOM con-

centration and the theoretical concentration calculated from the physical mixing line. The DOC and DOP distributions generally exhibited a deficit with respect to the theoretical mixing regression at low salinity (Fig. 7A,E). In contrast, there is a significant DOC excess ( $p < 0.01$ ) at salinities higher than 30 (more variable for DOP). As for other parameters (e.g. bacterial and phytoplanktonic production), there were anomalies in the DOC distribution during the spring bloom (Biodypar

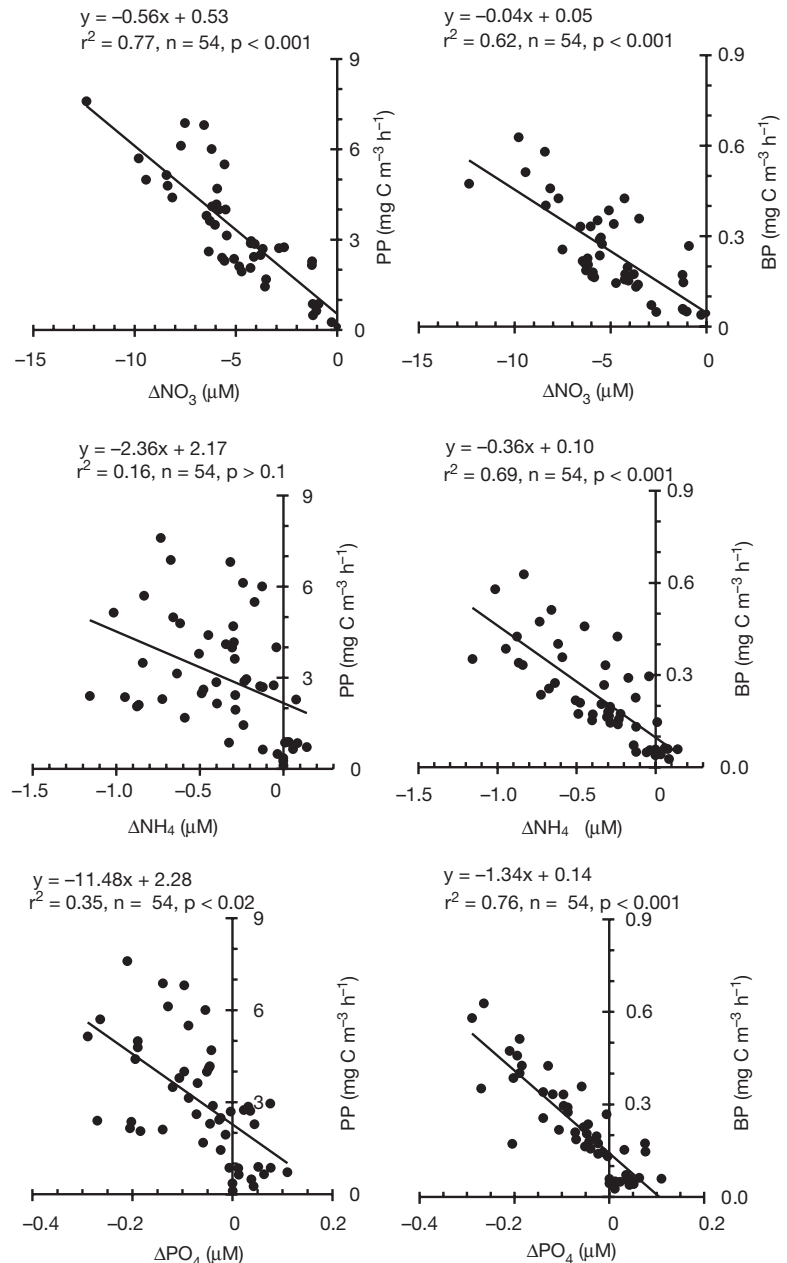


Fig. 6. Relationship between uptake of nutrients ( $\Delta\text{NO}_3$ ,  $\Delta\text{NH}_4$ ,  $\Delta\text{PO}_4$ ) and primary production (PP) or bacterial production (BP) for Biodypar Cruise 4 (both trajectory D112 and D120); the linear least-square regression (formula and statistics) is indicated on each panel

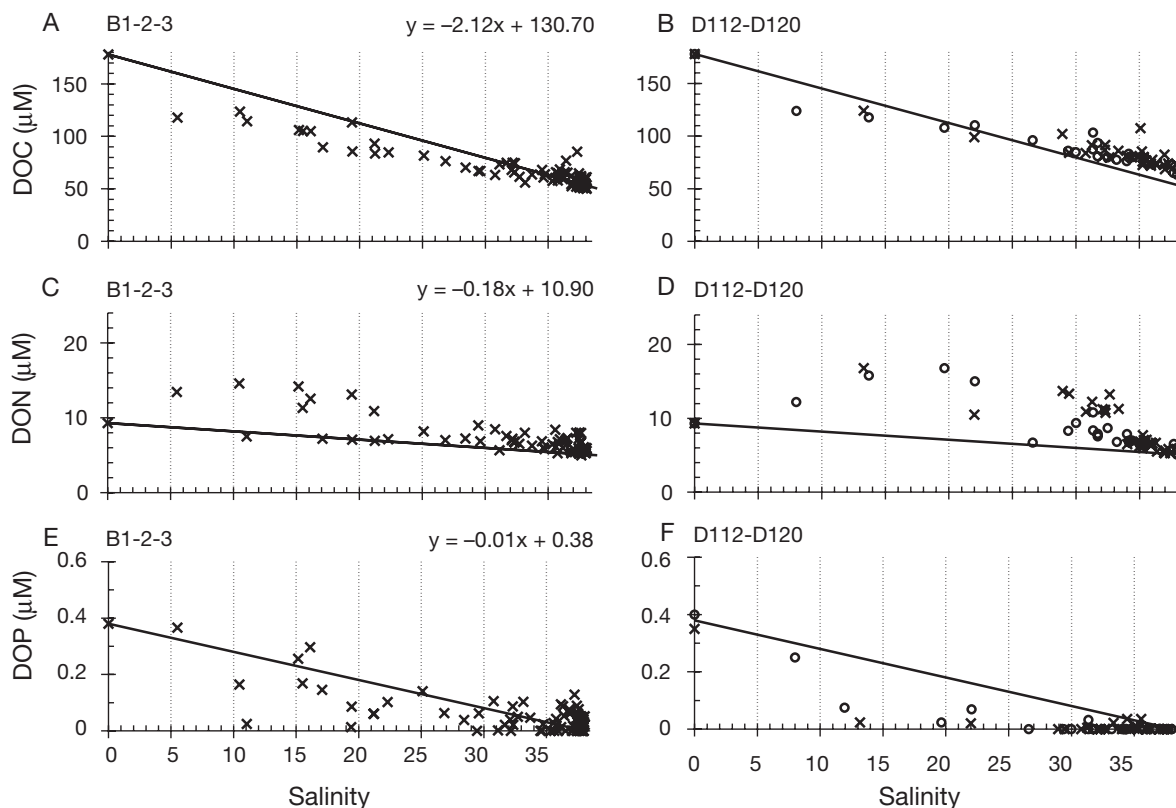


Fig. 7. Evolution of DOC, DON and DOP along the salinity gradient in the Rhône River plume. (A,C,E) B1-2-3 = Biodypar Cruises 1, 2 and 3; (B,D,F) D112-D120 = Biodypar Cruise 4. The equations of the theoretical mixing model line for DOC, DON and DOP are indicated (see text for details)

Cruise 4), but the general trend remained the same for DOC, albeit shifted towards lower salinity (Fig. 7B). DOP concentrations became rapidly undetectable along the salinity gradient (Fig. 7F). The pattern of DON was quite different and characterised by a systematic excess of DON along the salinity gradient (Fig. 7C, D).

## DISCUSSION

Collection of data along different trajectories enables a detailed description of the horizontal and vertical morphology of the Rhône River plume. Indeed, the riverine discharge into the Gulf of Lion forms a visible plume of turbid water 1 to 2 m thick that extends a few tens of kilometres seaward. The plume layer contains fresh nutrient-rich water and overlies the nutrient-poor seawater layer. The general dynamics and hydrological fields of this system are described in Broche et al. (1998), where simultaneous examination of radar maps and Lagrangian drifter tracking allowed the main dynamic tendencies of the Rhône River plume to be resolved. The spatial and temporal spreading of the plume is mainly controlled by meteorological factors and river discharges. Usually, wind stress appears as the dominant parameters in this evolution. For example, within a few hours the structure of the plume can evolve from a large bi-layer structure to a thick homogeneous or complex multi-layer structure (Naudin

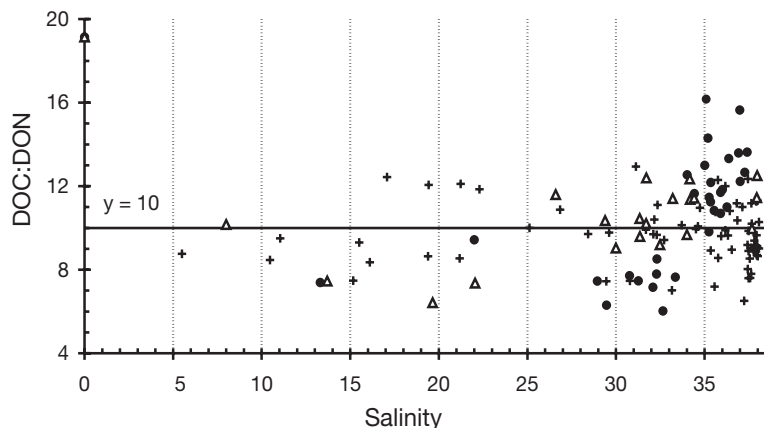


Fig. 8. Changes in the DOC:DON ratio along the salinity gradient. (+) = Biodypar Cruises 1, 2 and 3; (●) = Biodypar Cruise 4 D112; (Δ) = Biodypar cruise 4 D120. The horizontal line shows the threshold value of 10

et al. 1997). Mixing conditions between freshwater and marine water induce complex events like dilution, flocculation, or aggregation (Thill et al. 2001). Introduction of freshwater flow into this marine environment induced a strong salinity gradient under all flow rates recorded during the Biodypar cruises. Off the river mouth the spreading of the plume favours dilution processes. Nutrients and DOM generally decreased and vary inversely with salinity while inputs from the river were directly mixed into the coastal autochthonous material (Naudin et al. 2001). In fact, the distribution of these dissolved elements within the plume is not only a function of riverine inputs and physical mixing processes, but also depends on all other processes which add or remove nutrients, especially through biological activities. Biological uptake removes nutrients from seawater, whereas bacterial activity could add (regeneration) and/or remove (consumption) nutrients from seawater.

The study of linear relationships along the gradient of salinity gave a good estimate of the respective role of physics and biology in the dilution process. Indeed, for each Biodypar cruise, concentrations of nutrients and DOM were plotted against salinity to investigate whether the transport of these elements into the dilution area was conservative or not. These relationships, widely used in estuarine surveys (Fox 1990, Benner & Opsahl 2001) for data interpretation, are discussed in different works (Broenkow 1965, Minas et al. 1974, Morin et al. 1985, Naudin et al. 2001). During Biodypar Cruises 1, 2, and 3, linear least-square regression fits of  $\text{NO}_3$ ,  $\text{NH}_4$ , and  $\text{PO}_4$  versus salinity were typically consistent with the predominance of a conservative mixing which indicates the dominance of physical dilution for most of the year (i.e. at least between November and March). As a consequence, nutrient inputs are not used in the dilution area but are dissipated into nutrient poor marine water. Significant deviations in the property-salinity plots from this linear relation during the Biodypar Cruise 4 indicate a non-conservative mixing relationship (Fig. 2). Physical dilution during this period is no longer the dominant removal process and, as the net budget represents the balance between all of the biotic and abiotic processes taking place, we can assume that these deviations were mainly attributed to biological activities, such as consumption (uptake) and/or production. In relation to the phytoplankton bloom development, departure from the theoretical conservative mixing rate took about 1 wk to increase by a factor of 2 during our sampling period. High phytoplankton and bacterial productivity during the bloom period accounted for the relative depletion of  $\text{NO}_3$ ,  $\text{PO}_4$  or  $\text{NH}_4$  at intermediate salinity. Biological impacts were thus increasingly important compared to physical dilution, especially because high transfer

rates (e.g. turbulence, current, river discharge) progressively decreased at that time.

The dominant role of biological uptake over the other processes during the phytoplankton bloom can be supported by invoking the Redfield atomic N:P ratio of 16:1 for phytoplankton or of 10:1 for bacteria (Fagerbakke et al. 1996), and by comparing the  $\Delta\text{N}:\Delta\text{P}$  ratio (Table 1). There was a clear increase in the disappearance (considered as uptake) of all nutrients between the 2 trajectories D112 and D120 of the Biodypar Cruise 4 (more than 60%), but no strong variations were observed in the N:P ratios of these uptakes. If the nutrient changes were closely associated with phytoplankton and bacterial uptake, their ratios should be close to the ratio predicted by Redfield if we hypothesize a non-limiting status by nutrients. The integrated uptake ratio,  $\text{I}\Delta\text{NH}_4:\text{I}\Delta\text{PO}_4$ , of 2.2 is close to the value proposed for bacterial uptake. When the uptake of  $\text{NH}_4$  and  $\text{NO}_3$  are combined, the resulting ratio ( $\text{I}\Delta\text{NO}_3+\text{I}\Delta\text{NH}_4:\text{I}\Delta\text{PO}_4$ ) of 13 to 14 is close to the Redfield ratio, but far from the classical mineral ratio of 22 in deep Mediterranean seawater. With an initial mineral N:P ratio of 65 to 70 in the Rhône maintained during the physical dilution processes, the terrestrial inputs largely contribute to an increase in the known phosphate depletion of the Mediterranean Sea.

The distribution of phytoplankton and bacteria populations depends upon numerous factors such as their salinity tolerance, the condition of the physical and chemical environment, as well as competition for key resources and predator-prey relationships. Horizontal and vertical salinity gradients in the Rhône plume had an important inhibitory effect on biological activities (Riley 1937) such as photosynthesis and growth of phytoplankton species (Cloern 1978, Miller & Kamykowski 1986). The variation in temperature, light, and quantity of suspended particles generally play a minor role on biological activity relative to the short mixing time of surface water (Naudin et al. 2001). The variation in intensity of some key environmental factors, like wind and outflow, are fundamental for biological activity. This can be illustrated during our study with the inter-annual variation in the timing of production, well known in the Mediterranean Sea (Lefèvre et al. 1997). Wind stress and general circulation forcing usually decrease in spring (Conan & Millot 1995) and allow the stratification of the water column. However, one can assume that the development of the phytoplankton bloom in April 1999 but not in April 1998, was related to more favourable environmental conditions, especially upon the outflow variability of the Rhône River and the prevailing wind conditions. Effectively, during the Biodypar Cruise 4, wind and outflow were both lower than during the Biodypar Cruise 1 (outflow  $>2500$  but  $<2000$   $\text{m}^3 \text{s}^{-1}$  and wind (SE)  $>4$   $\text{m s}^{-1}$  but

quasi-non existent or  $<1 \text{ m s}^{-1}$  during Biodypar Cruises 1 and 4, respectively).

In the Rhône mixing zone, microplankton represented 50% of the chlorophyll *a* and primary production (Owens et al. 1989, Videau & Leveau 1990), and, it is a region of high productivity (Lefèvre et al. 1997, Conan et al. 1999, Thill et al. 2001) like other river plume systems (e.g. Mississippi River plume, Lohrenz et al. 1990, Gulf of Papua, Davies 2004). This interface is also associated with high concentrations of micro-zooplankton (Gaudy 1990). During the Biodypar Cruise 4, a significant enhancement of bacterial abundance and chlorophyll concentration, as well as production, were measured in the salinity range 29 to 36 (trajectory D112) and 26 to 34 (trajectory D120) (Fig. 4). The salt tolerance of the populations, and the light limitation in the turbid part of the plume contrasting with a nutrient-limited area at seaward sites were among the factors responsible for this distribution (Colijn & Cadée 2003). At low salinity, nutrient limitation rarely occurs, and irradiance and turbulence act as the major limiting factors on productivity. It has been reported that phytoplankton are able to largely acclimate to high nitrate levels by increasing their uptake capacity, which could ultimately override the effect of other variables; including irradiance, temperature, and cell size (Collos et al. 2005). This result minimizes the potential negative effect of high nutrient concentration on biological uptake and on spatial organisation of the ecosystem in the dilution area.

During the Biodypar Cruise 4, maximum phytoplanktonic biomass and primary production followed maximum bacterial abundance and production in the salinity gradient. This distribution is frequently found between bacteria and phytoplankton in marine ecosystems, and could result from bacterial utilization of substrates introduced by the river (Kirchman et al. 1989), as well as from autochthonous material originated from phytoplankton (White et al. 1991). During the Biodypar Cruise 4, environmental conditions and biological activities favoured a spatial (along the haline gradient) and temporal (along the trajectory) discrimination of nutrient uptake. These conditions explained the typical association between maximum phytoplanktonic biomass, production and highest  $\text{NO}_3$  consumption rates, as well as between maximum bacterial abundance, production and  $\text{NH}_4$  and  $\text{PO}_4$  consumption rates (Figs. 3 & 4). Heterotrophic bacteria have high affinity for  $\text{PO}_4$  and  $\text{NH}_4$  and they often account for a large proportion of the total uptake of these elements in freshwater and marine environments (Kirchman 1994). Less clear are the factors controlling the relative uptake by bacteria and its consequences on the planktonic community. During the Biodypar Cruise 4, an important competition between phytoplankton and bacteria for available nutrients resulted in the variability of both

the temporal and spatial distribution of both groups and their relative activities. Indeed, primary production in the dilution area is fuelled in part by the supply of regenerated nitrogen in support of new production (Wawrik & Paul 2004), and there is a competition for key nutrients (Yin et al. 2004).

The case of DOM is slightly different from that of inorganic nutrients as during all cruises, production and consumption processes are always observed in addition to a conservative dilution (Fig. 7). In marine temperate areas, a surface DOM accumulation at the end of the summer could result from a competition for available nutrients, as nitrogen or phosphorus (Thingstad et al. 1997, Pujó-Pay & Conan 2003). It is clear that  $\text{PO}_4$  concentration rapidly dropped compared to other nutrients (Fig. 2), quickly reaching low or undetectable values during the Biodypar Cruise 4. It is also the case for DOP reaching rapidly undetectable concentrations along the salinity gradient. Moreover, the DIN:DIP ratio of about 60 in the Rhône indicated a potential  $\text{PO}_4$  depletion. Also, the encountered DOM accumulation resulted from short term processes originating from the phytoplankton bloom at the salinity end range (Fig. 7). This pool has been shown to be degradable for 18 to 100% in 20 d (Déliat et al. in press). In the dilution area of the plume, the major part of the labile DOM had an autochthonous origin as previously reported. Similar results were found in the Pearl River estuarine coastal plume, where phosphate addition in water samples was necessary to consume all the nitrogen (Yin et al. 2004).

Changes in the DOC:DON ratio along the salinity gradient (Fig. 8) suggest that there is potential competition for key nutrients (especially for nitrogen) between bacteria and phytoplankton within the mixing zone. Indeed, previous works have shown that a C:N ratio of 10 for the DOM pool is a strong threshold value (e.g. Goldman et al. 1987, Anderson 1992). Below this ratio, bacteria meet their nitrogen requirement for growth and so bacteria are a source of ammonia for the ecosystem (ammonification process). Up to a ratio of 10, bacteria need to consume nitrogen to equilibrate their internal ratio and bacteria will consume DIN (preferentially  $\text{NH}_4$ ). Also, nitrogen could rapidly become a limiting factor and result in DOC accumulation. This phenomenon was proposed by Pujó-Pay and Conan (2003) as being responsible for summer DON accumulation in the surface water of the Gulf of Lion through phosphate limitation of the ecosystem. During the current study, the DOC:DON ratio was initially high in Rhône River water (about 19) and then decreased to  $<10$  at salinities of 5 to 20 (Fig. 8). This ratio remained stable and wavered between 7 and 13 for higher salinities during Biodypar Cruises 1, 2, and 3, but increased up to 15 during the spring bloom of the Biodypar Cruise 4. In comparing this evolution with

the distribution of DOC concentration shown in Fig. 7, it appeared that a DOC:DON ratio <10 corresponded to a DOC concentration distributed below the theoretical physical dilution line, indicating net consumption. Whereas a DOC:DON ratio >10 corresponded to an increase of DOC concentrations and then an accumulation. The importance of the DOM pool, in terms of production and consumption, was previously encountered in the dilution area of the Fly River in the Gulf of Papua (Davies 2004). Within the Fly plume, primary productivity appeared to rely on recycled nutrients, with organic fractions representing the majority of the nutrient pool. Basically, the plume is characterised by remineralisation of organic matter, but during drought conditions DON production and ammonium uptake suggest that bacterial activity is more prevalent.

In conclusion we find that the Rhône River plume is an extremely dynamic environment that responds to the variations of the river inputs and the physical forcing on short (hours to day) to longer time scales (week to season and year). In our study, there was a clear evolution between a system where physical mixing processes were dominant (most of the time during winter), and a system (Biodypar Cruise 4) characterised by a phytoplankton bloom where biological processes, such as production and uptake, progressively overrode the physical mixing. Light and nutrients are critical limiting factors for production in the Rhône River plume, but additional constraints also contribute to the observed pattern of biomass and production along the Rhône River plume/oceanic gradient. At high salinity, it is likely that biomass and production are constrained by a reduction in nutrient supply. At intermediate salinity, nutrients are adequate to support growth beyond observed levels but the control of biomass and production is more complex and need to include chemical and physical factors. The study of the various ratios of the principal elements (C:N:P) would also need further investigation to understand the balance between production and uptake. Our study finally helped to better elucidate the control of the productivity of the Rhône River plume area. It seems that studies in the mixing area in a range of salinity of 26 to 36 are essential to quantify the impact of the productivity of this system and to quantify the impact of the river discharge on a more global scale. In addition to seasonal variations, it is essential to consider the time of mixing within the plume, which is largely controlled by conditions of wind and riverine outflow.

*Acknowledgements.* This research was supported by the 'Programme National Environnement Côtier'. We thank M. J. Behrenfeld for his helpful comments and we are grateful to A. P. Rees for his help in correcting the English language in the final manuscript. Finally, we thank the Captains and crews of the RV 'Tethys' for their help during seawork.

#### LITERATURE CITED

- Anderson TR (1992) Modelling the influence of food C:N ratio, and respiration on growth and nitrogen excretion in marine zooplankton and bacteria. *J Plankton Res* 14: 1645–1671
- Arnoux-Chiavassa S, Fraunié P (2003) Modeling 3D Rhône River plume using a higher order advection scheme. *Oceanol Acta* 26:299–309
- Benner R, Opsahl S (2001) Molecular indicators of the sources and transformations of dissolved organic matter in the Mississippi River plume. *Org Chem* 32:597–611
- Broche P, Devenon JL, Forget P, De Maistre JC, Naudin JJ, Cauwet G (1998) Experimental study of the Rhône plume Part I: physic and dynamics. *Oceanol Acta* 21:725–738
- Broenkow WW (1965) The distribution of nutrients in the Costa Rica Dome in the eastern Tropical Pacific Ocean. *Limnol Oceanogr* 10:40–52
- Cauwet G (1994) HTCO method for dissolved organic carbon analysis in sea water: influence of catalyst on blank estimation. *Mar Chem* 47:55–64
- Cloern JE (1978) Empirical model of *Skeletonema costatum* photosynthetic rate, which applications in the San Francisco Bay estuary. *Adv Water Resour* 1:267–274
- Colijn F, Cadée GC (2003) Is phytoplankton growth in the Wadden Sea light or nitrogen limited? *J Sea Res* 49:83–93
- Collos Y, Vaquer A, Souchu P (2005) Acclimatation of nitrate uptake by phytoplankton to high substrate levels. *J Phycol* 41:466–478
- Conan P, Millot C (1995) Variability of the Northern Current off Marseilles, Western Mediterranean Sea, from February to June 1992. *Oceanol Acta* 18:193–205
- Conan P, Pujo-Pay M, Raimbault P, Leveau M (1998) Variabilité hydrologique et biologique au sein du Courant Nord Méditerranéen à l'entrée du golfe du Lion. I. Bilan annuel des transports en azote et productivité potentielle. *Oceanol Acta* 21:751–765
- Conan P, Turley CM, Stutt E, Pujo-Pay M, Van Wambeke F (1999) Relationship between phytoplankton efficiency and the proportion of bacterial production to primary production in the Mediterranean Sea. *Aquat Microb Ecol* 17: 131–144
- Coste B (1974) Role des apports nutritifs minéraux rhodaniens sur la production organique des eaux du golfe du Lion. *Tethys* 6:727–740
- Davies P (2004) Nutrient processes and chlorophyll in the estuaries and plume of the Gulf of Papua. *Cont Shelf Res* 24:2317–2341
- Déliat G, Cauwet G, Pujo-Pay M, Oriol L, Conan P, Naudin JJ (in press) Dissolved organic matter in the Rhône River plume: origin and biodegradability. *Mar Chem*
- Estournel C, Broche P, Marsaleix P, Devenon J, Auclair F, Vehil R (2001) The Rhône River plume in unsteady conditions: numerical and experimental results. *Estuar Coast Shelf Sci* 53:25–38
- Fagerbakke KM, Heldal M, Norland S (1996) Content of carbon, nitrogen, oxygen, sulfur and phosphorus in native aquatic and cultured bacteria. *Aquat Microb Ecol* 10: 15–27
- Fitzwater SE, Knauer GA, Martin JM (1982) Metal contamination and its effect on primary production measurements. *Limnol Oceanogr* 27:544–551
- Fox (1990) Geochemistry of dissolved phosphate in the Sepik River and Estuary, Papua, New Guinea. *Geochim Cosmochim Acta* 54:1019–1024
- Fuhrman JA, Azam F (1982) Thymidine incorporation as a measure of heterotrophic bacterioplankton production in

- marine surfaces waters: evaluation and field results. *Mar Biol* 66:109–120
- Gaudy R (1990) Zooplankton feeding on seston in the Rhône River plume area (NW Mediterranean Sea) in May 1988. *Hydrobiol* 207:241–249
- Goldman JC, Caron DA, Dennett MR (1987) Regulation of gross growth efficiency and ammonium regeneration in bacteria by substrate C:N ratio. *Limnol Oceanogr* 32:1239–1252
- Kirchman DL (1994) The uptake of inorganic nutrients by heterotrophic bacteria. *Microbiol Ecol* 28:255–271
- Kirchman DL, Soto Y, Van Wambeke F, Bianchi M (1989) Bacterial production in the Rhône River plume: effect of mixing on relationship among microbial assemblages. *Mar Ecol Prog Ser* 53:267–275
- Koroleff F (1969) Direct determination of ammonia in natural waters as indophenol blue. *Int Council Explor Sea C9*:19622
- Lee S, Furchman JA (1987) Relationships between biovolume and biomass of naturally derived marine bacterioplankton. *Appl Environ Microbiol* 53:1298–1303
- Lefèvre D, Minas HJ, Minas M, Robinson C, Williams PJL, Woodward EMS (1997) Review of gross community production, primary production, net community production and dark respiration in the Gulf of Lions. *Deep-Sea Res* 44:801–832
- Lohrenz SE, Dagg MJ, Whittedge TE (1990) Enhanced primary production at the plume/oceanic interface of the Mississippi River. *Cont Shelf Res* 7:639–664
- Miller RL, Kamykowski DL (1986) Short-term photosynthetic responses in the diatom *Nitzschia americana* to a simulated salinity environment. *J Plankton Res* 8:305–315
- Minas HJ, Minas M (1989) Primary production in the Gulf of Lions with considerations to the Rhône River inputs. In: Martin JM, Barth H (eds) *Water pollution research report EROS 2000, 13*, Commission of the European Communities. E Guyot, Brussels, p 112–125
- Minas HJ, Romana LA, Packard TT, Bonin MC (1974) Oxygen distribution in a coastal upwelling (Northwest Africa) and in the Costa Rica dome. *Tethys* 6:157–170
- Morin P, Le Corre P, Le Fèvre J (1985) Assimilation and regeneration of nutrients off the west coast of Brittany. *J Mar Biol Assoc UK* 65:677–695
- Naudin JJ, Cauwet G, Chretiennot-Dinet MJ, Deniaux B, Devenon JL, Pauc H (1997) River discharge and wind influence upon particulate transfer at the land-ocean interaction. Case study of the Rhone river plume. *Estuar Coast Shelf Sci* 45:303–316
- Naudin JJ, Cauwet G, Fajon C, Oriol L, Terzic S, Devenon JL, Broche P (2001) Effect of mixing on microbial communities in the Rhône River plume. *J Mar Syst* 28:203–227
- Neveux J, Panouse M (1987) Spectrofluorometric determination of chlorophylls and pheophytin. *Arch Hydrobiol* 109:567–581
- Owens NJP, Rees AP, Woodward EMS, Mantoura RFC (1989) Size-fractionated primary production and nitrogen assimilation in the north-western Mediterranean Sea during January 1989. In: Martin JM, Barth H (eds) *Water pollution research report EROS 2000, 13*, Commission of the European Communities. E Guyot, Brussels, p 126–135
- Parsons TR, Maita Y, Lalli CM (1992) *A manual of chemical and biological methods for seawater analysis*. Pergamon Press, New York
- Platt T, Sathyendranath S (1993) Fundamental issues in measurement of primary production. In: ICES Marine Sciences Symposium, Vol 197, La Rochelle
- Pujo-Pay M, Conan P (2003) Seasonal variability and export of dissolved organic nitrogen in the North Western Mediterranean Sea. *J Geophys Res* 108:1901–1911
- Pujo-Pay M, Raimbault P (1994) Improvement of the wet-oxidation procedure for simultaneous determination of particulate organic nitrogen and phosphorus collected on filters. *Mar Ecol Prog Ser* 105:203–207
- Pujo-Pay M, Conan P, Raimbault P (1997) Excretion of dissolved organic nitrogen by phytoplankton assessed by wet oxidation and <sup>15</sup>N tracer procedures. *Mar Ecol Prog Ser* 153:99–111
- Riley GA (1937) The significance of the Mississippi River drainage for biological conditions in the northern Gulf of Mexico. *J Mar Res* 1:60–74
- Servais P, Lavandier P (1995) Mesure de la production bactérienne par incorporation de thymidine et de leucine marquées: discussion des protocoles expérimentaux et exemples d'application. *Oceanis* 21:161–189
- Steemann-Nielsen E (1952) The use of radio-active (C<sup>14</sup>) for measuring organic production in the sea. *J Cons Int Explor Mer* 18:117–140
- Sugimura Y, Suzuki Y (1988) A high temperature catalytic oxidation method for the determination of non-volatile dissolved organic carbon in sea water by direct injection of a liquid sample. *Mar Chem* 24:105–131
- Thill A, Moustier S, Garnier JM, Estournel C, Naudin JJ, Bottero JY (2001) Evolution of particle size and concentration in the Rhône River mixing zone: influence of salt flocculation. *Cont Shelf Res* 21:2127–2140
- Thingstad TF, Hagström Å, Rassoulzadegan F (1997) Accumulation of degradable DOC in surface waters: is it caused by a malfunctioning microbial loop? *Limnol Oceanogr* 42:398–404
- Tréguer P, Le Corre P (1975) *Manuel d'analyses des sels nutritifs dans l'eau de mer*. Laboratoire d'Océanographie Chimique, Université de Bretagne Occidentale, Brest
- Videau C, Leveau M (1990) Phytoplanktonic biomass and productivity in the Rhône River plume in the spring time. *C R Acad Sci* 311:219–224
- Wawrik B, Paul JH (2004) Phytoplankton community structure and productivity along the axis of the Mississippi River plume in oligotrophic Gulf of Mexico waters. *Aquat Microb Ecol* 35:185–196
- White PA, Kalff J, Rasmussen JB, Gasol JM (1991) The effect of temperature and algal biomass on bacterial production and specific growth rate in freshwater and marine habitats. *Microb Ecol* 21:99–118
- Yin K, Song X, Sun J, Wu MCS (2004) Potential P limitation leads to excess N in the pearl river estuarine coastal plume. *Cont Shelf Res* 24:1895–1907
- Yoro SC, Sempéré R, Turley CM, Unanue MA, Durrieu de Madron X, Bianchi M (1997) Cross-slope variations of organic carbon and bacteria in the Gulf of Lions in relation to water dynamics (Northwestern Mediterranean). *Mar Ecol Prog Ser* 161:255–264